Int. J. Solids Structures Vol. 24, No. 6, pp. 567–580, 1988
Printed in Great Britain.

0020–7683/88 $3.00 + .00

DAMAGE EVOLUTION AND RUPTURE IN CREEPING OF POROUS MATERIALS

J. TIROSH† and A. MILLER
Department of Materials Science and Engineering, Stanford University, Stanford, CA 94305, U.S.A.

(*Received* 19 *February* 1987; *in revised form* 20 *July* 1987)

Abstract—The configurational evolution in time and space of two-dimensional ellipsoidal damage into an elongated flaw with preferred orientation is solved and studied. The damage is represented as a single, traction free, ellipsoidal void embedded in an infinitely large time-dependent porous-like solid. The solid creeps in a power-law fashion under static biaxial loads which induce a large-scale rotation (with volume enlargement contraction) of the void. In the special case of unidirectional loading the free boundary of the void evolves into an expanded and elongated new shape while rotating towards a position codirectional with the principal tensile axis. The solution which describes this phenomenon made use of the analogy between linear viscous fluid and incompressible elasticity but has been extended (by incremental time-step integration) to geometrical and material nonlinearities. The enlargement of the analysis to multiple-voids interactions (via the "self-consistent" approximation) enables one to follow the porosity time evolution till rupture. The main outcome is the reinforcement of McClintock and Berg's vision of the ductile rupture mechanism by void coalescence. The process simulation agrees well with visual observations of void expansion and rotation in a highly viscous material and with experimental measurements of the rupture ductilities of creeping materials with different strain-rate sensitivity index. Similarities and dissimilarities with existing phenomenological damage theories are discussed.

1. INTRODUCTION

Structural materials contain, inevitably, a certain number of voids. For some engineering applications such porous material is beneficial (e.g. for slide bearing cages, for shock wave attenuation, etc.) but for the purpose of load carrying capacity, the porosity is detrimental. For creeping materials, in particular, voids may shorten substantially the lifetime for rupture failure at a given holding load. This issue is examined in this paper.

The physical phenomenon of rupture of creeping materials may, for the purpose of clarity, be divided into three stages: (a) nucleation of cavities in a form of micro-voids, (b) steady-state growth of the voids, and (c) rupture by the coalescence of the voids. Each of the stages is supposedly controlled by a different physical mechanism. Although coupling between various mechanisms is conceived[1], the growth and coalescence stages are primarily dominated by continuum creep mechanisms and encompass most of the lifetime of the solid prior to rupture. Our analysis can therefore start from a given volume fraction of an array of voids equally spaced throughout the body, and proceeds by observing their rotation and growth during creep under remote static loading. Rupture may then be defined when a representative void reaches a certain dimension, say, half the distance to the adjacent void, or perhaps more precisely, when the ligament between voids contracts to zero, so defined in this work.

A detailed study of the growth of a single void in a linear rigid plastic solid was considered by McClintock[2], Rice and Tracey[3], and in a linear viscous solid by Berg[4]. Their solutions have been unified and enlarged by Budiansky *et al.*[5] to encompass the power-law constitutive behavior of the materials. It appears, time and again, that the void growth behavior is highly sensitive to a hydrostatic stress environment.

In addition to the above study two more features seem essential to consider.

(a) The role of rotation of an ellipsoidal void, noted first by Berg[4], in hampering/enhancing its growth rate.

† On leave from Technion, Israel Institute of Technology, Faculty of Mechanical Engineering, Haifa, Israel.

(b) The interaction between voids (in a "self-consistent" fashion) akin to the study of ductile rupture by multi-voids coalescence. The rupture simulation based on (a) and (b) agrees qualitatively with visual observation of void growth and partially with other solutions[6–8].

The mathematical procedure employed here is based on the Rayleigh analogy between solutions related to *linear* elastic and *linear* viscous solid problems. Aided by Muskhelishvili's[9] elastic solution, a direct relationship between the prescribed load and the velocities of the void-free boundary is gained. This relationship, linear for an arbitrary small time interval, is integrated throughout the time history of the creeping process with continuous updating of the material (non-linear) properties and the large (non-linear) geometrical changes of the void configuration. The procedure appears efficient and highly cost effective compared to, say, FEM solutions of a similar nature[8] (the CPU time for a typical simulation of void growth until rupture under holding load is of the order of 1 min on an IBM 3084).

2. CONSTITUTIVE EQUATION AND RATE MEASURES

Consider an unbounded solid with the following time-rate response

$$\sigma = C(\dot{\varepsilon})^n, \qquad 0 \leqslant n \leqslant 1 \tag{1}$$

where C and n are material properties and σ and $\dot{\varepsilon}$ are the non-dimensional effective stress and strain rate fields normalized with respect to predetermined reference values σ_0 and $\dot{\varepsilon}_0$, i.e. $\sigma = \tilde{\sigma}/\sigma_0$, $\dot{\varepsilon}_0 = \tilde{\dot{\varepsilon}}/\dot{\varepsilon}_0$. If one chooses $\dot{\varepsilon}_0$ to be the steady-state strain rate corresponding to the applied stress σ_0 then $C = 1$ (identically) in eqn (1). σ and $\dot{\varepsilon}$ are defined in terms of their tensorial components (normalized too, as above) by their invariant form as

$$\sigma = (3/2 s_{ij} s_{ij})^{1/2}, \qquad s_{ij} = \sigma_{ij} - \frac{1}{3}\delta_{ij}\sigma_{kk} \tag{2}$$

$$\dot{\varepsilon} = (2/3 \dot{\varepsilon}_{ij}\dot{\varepsilon}_{ij})^{1/2}, \qquad \dot{\varepsilon}_{ij} = \frac{1}{2}(u_{i,j} + u_{j,i}) \tag{3}$$

where u_i is the velocity field at the considered point. Time integration of eqns (3) represents the total strain history as

$$\varepsilon_{ij} = \int_0^t \dot{\varepsilon}_{ij}\, \mathrm{d}t. \tag{4}$$

The equivalence of eqn (1) in tensorial form can be shown to be

$$\dot{\varepsilon}_{ij} = (3/2)^{\frac{(1-n)}{2}} \frac{\dot{\varepsilon}^{(1-n)}}{C} s_{ij} \qquad (0 \leqslant n \leqslant 1). \tag{5}$$

Perfectly plastic solids ($n = 0$) and linear viscous solids ($n = 1$) are, as indicated, the extreme values of exponent n. Equation (5) can be written as

$$\dot{\varepsilon}_{ij} = \frac{1}{2\eta} s_{ij} \tag{6}$$

so that the parameter η represents the viscosity of the solid defined from eqn (5) as

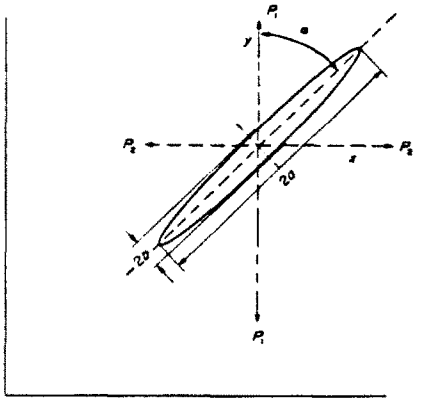

Fig. 1. The geometry of an elliptical void and its orientation with respect to the principal (vertical) load.

$$\eta(\dot{\varepsilon}) = (1/3)C(\dot{\varepsilon})^{n-1}. \tag{7}$$

Let an isolated elliptical two-dimensional void be embedded in the solid, such that its major axis is oriented at an angle α_0 to the far-field principal stress direction (Fig. 1). First we will assume that the volume comprising the void is negligible compared with the volume of the solid so that the uniformity of the field σ_{ij}, $\dot{\varepsilon}_{ij}$ away from the void is (nearly) unperturbed (this restriction will be relaxed later when porosity considerations are introduced). The three independent geometrical variables which completely define the current void configuration were chosen (for convenience) to be:

the "eccentricity";	$m = (a-b)/(a+b)$,	$0 \leqslant m < 1$
the "perimeter";	$R = (a+b)/2$,	$R > 0$
the "orientation";	α = major axis orientation,	$0 \leqslant \alpha \leqslant 90°$.

(8)

Associated parameters are the aspect ratio $\lambda = a/b$, and time-growth rates ($\dot{\lambda}$, $\dot{a}$, $\dot{b}$, $\dot{m}$, etc.) derived with respect to a normalized time, t, namely

$$t = \hat{t} \cdot \dot{\varepsilon}_0. \tag{9}$$

During the creeping process the velocity field of the void's free surface, $u_i(s)$ (derived next), is used repeatedly to update the void configuration at small time increments. The local strain-rate field $\dot{\varepsilon}_{ij}^{(c)}$ associated with the motion $u_i(s)$ of the void surface S_c is

$$\dot{\varepsilon}_{ij}^{(c)} = \frac{1}{V_c}\int_{V_c}\frac{1}{2}(u_{i,j}+u_{j,i})\,\mathrm{d}V_c = \frac{1}{V_c}\int_{S_c}\frac{1}{2}(u_i n_j + u_j n_i)\,\mathrm{d}S \tag{10}$$

via the divergence theorem.

Assuming that the evolving shape of the void retains its ellipsoidal form, the principal strain rate of eqn (10) is

$$\dot{\varepsilon}_b^{(c)} = \dot{b}/b,\ \dot{\varepsilon}_a^{(c)} = \dot{a}/a \tag{11}$$

so that a measure of the effective strain rate, attributed to the void evolution in the plane-stress case, is reduced to

$$\bar{\varepsilon}^{(c)} = (2/\sqrt{3})\left((\dot{a}/a)^2 + (\dot{b}/b)^2 + (\dot{a}/a)(\dot{b}/b)\right). \tag{12}$$

3. ELASTIC SOLUTION—RECAPITULATION

Any remote static load applied on an infinite elastic two-dimensional body (with shear modulus μ) will produce a displacement field surrounding a traction-free cylindrical void of arbitrary shape by the following expression[9]:

$$u+iv = \frac{1}{2\mu}(\chi+1)\psi(z) \tag{13}$$

where

$$\chi = \begin{cases} 3-4\nu, & \text{for plane strain} \\ (3-\nu)/(1+\nu), & \text{for plane stress} \end{cases} \tag{14}$$

$\psi(z)$ is any analytic function of the variable $z = x+iy$ at the plane containing the void and having Poisson's ratio ν. The particular solution of the displacement field surrounding an ellipsoidal void subjected to bi-directional stresses at infinity, say P_1 and P_2, is constructed by enforcing $\psi(z)$ of eqn (13) to satisfy the pertinent boundary conditions.

Customarily (i.e. Ref. [9]) the known expression of $\psi(\xi)$ for a simpler circular void in an auxiliary plane, ξ, is utilized to get the proper expression for an ellipsoidal void via geometrical transformation from an auxiliary plane ξ into the physical plane z, namely

$$z = R(\xi + m/\xi) \tag{15}$$

so that the terminal solution (leaving aside the algebra involved) reads

$$\psi(\xi) = R\left(\frac{P_1+P_2}{4}\right)\left(\xi - \frac{m}{\xi}\right) + \left(\frac{P_1-P_2}{4}\right)R\frac{2e^{2i\alpha}}{\xi}. \tag{16}$$

Combining together eqns (13), (15) and (16) renders the exact relationship between the loading system, P_1 and P_2 and the induced displacement surrounding the void, provided the displacement is small enough not to perturb the solid behavior.

4. CREEP FLOW ANALOGY AND GEOMETRICAL NONLINEARITY

The analogy to creeping flow is based on the similarity between the constitutive equation of an incompressible elastic continua, namely

$$\varepsilon_{ij} = \frac{1}{2\mu}s_{ij} + \frac{\nu}{1-2\nu}\varepsilon_{kk}\delta_{ij} \tag{17}$$

where

$$\lim_{\nu \to 1/2} \varepsilon_{kk}\nu/(1-2\nu) \to 0 \quad \text{as} \quad \nu \to 1/2 \tag{18}$$

and the constitutive equation of linear viscous material described by eqn (6). By setting $\mu = \eta$, $\varepsilon_{ij} = \dot{\varepsilon}_{ij}$, and renaming the displacement field (u, v) in eqn (13) as the velocity field, the speed at which the void boundary is moving is described in an exact form, by eqns (16) and (13) as

$$u(s)+iv(s)=\frac{(\chi+1)}{2\eta}R\left[\left(\frac{P_1+P_2}{4}\right)\left(\xi-\frac{m}{\xi}\right)+\left(\frac{P_1-P_2}{4}\right)\frac{2e^{2i\alpha}}{\xi}\right] \tag{19}$$

for $\zeta = e^{i\phi}$ and $0 \leqslant \phi \leqslant 2\pi$.

After a short-time interval, Δt (short enough not to affect significantly solution (19) by variations in α, m or R), one should update the shape of the void by

$$\Delta z(s) = [u(s)+iv(s)]\Delta t. \tag{20}$$

Hence, the new shape $\hat{z}(s) = z(s)+\Delta z(s)$, based on eqns (15), (19) and (20), is rephrased as

$$\hat{z}(s) = R(1+\delta)\left(e^{i\phi}+e^{-i\phi}\left\{m\frac{1-\delta+\delta\left(\frac{P_1-P_2}{P_1+P_2}\right)\frac{2e^{2i\alpha}}{m}}{1+\delta}\right\}\right), \qquad 0<\phi<2\pi \tag{21}$$

where

$$\delta = \frac{(\chi+1)}{8\eta}(P_1+P_2)\Delta t.$$

Let us assume that the new configuration, $\hat{z}(s)$ *retains an ellipsoidal shape*, though with new variables $\hat{R}$, $\hat{m}$, $\hat{\alpha}$. The expression for this new ellipse is written most generally from eqn (15) as

$$\hat{z}(s) = \hat{R}(e^{i\phi}+e^{-i\phi}\,\hat{m}\,e^{2i\hat{\alpha}}). \tag{22}$$

The description of the ellipse by eqn (22), with the new variables $\hat{R}$, $\hat{m}$ and $\hat{\alpha}$, is equivalently described in eqn (21) in terms of the old variables R, m, α. Therefore, by comparing the terms of eqn (22) with those of eqn (21), one recognizes that the updated variables are related to their previous values by

$$\hat{R} = R(1+\delta) \tag{23}$$

$$\hat{m} = \text{complex absolute value of}\left\{m\frac{1-\delta+\delta\left(\frac{P_1-P_2}{P_1+P_2}\right)\frac{2e^{2i\alpha}}{m}}{1+\delta}\right\} \tag{24}$$

$$\hat{\alpha} = \frac{1}{2}\,\text{argument of}\left\{m\frac{1-\delta+\delta\left(\frac{P_1-P_2}{P_1+P_2}\right)\frac{2e^{2i\alpha}}{m}}{1+\delta}\right\}. \tag{25}$$

Equations (23)–(25) constitute the basic algorithm for the numerical tracking of the ellipsoidal damage evolution. After each time step, Δt ("hidden" in δ), the ellipse gets a slightly different configuration according to eqns (23)–(25), beyond a certain creeping time the simulation is terminated. As a typical example, a time history simulation of void rotation and expansion in a power law creeping material for unidirectional tension is shown in Fig. 2. A visual observation in Fig. 3, using "silly putty" material (commercial name for a highly time-dependent synthetic compound) validates phenomenologically the suggested solution of Fig. 2. When the load is reversed from unidirectional tension (P_1) to unidirectional

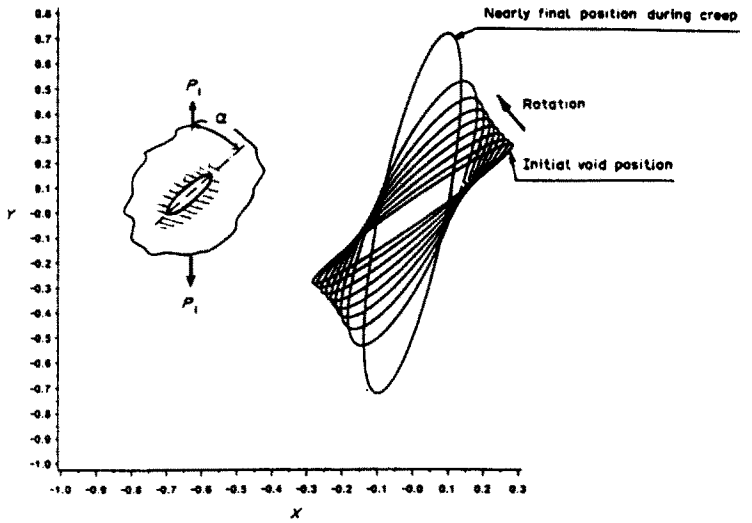

Fig. 2. The simultaneous void rotation and expansion during a power-law creep ($n = 0.5$) at a constant (vertical) load solved by eqns (21)–(25).

compression ($-P_1$) the rotation of the voids is also reversed but not at the same rate (as is evident from Fig. 4) and the void is eventually contracted into a narrow slit.

5. SELF-CONSISTENT SOLUTION

Consider a sample of visco-plastic solid which contains equally distributed voids, all of which have the same ellipsoidal size and orientation. The volume fraction of the voids is, of course, a time-dependent variable and denoted as f. Let us define a characteristic unit cell of volume V in the body which comprises a single void (with volume $V^{(c)}$) and surrounding matrix of volume $V^{(m)}$ such that

$$V^{(m)} = V - V^{(c)}. \tag{26}$$

The volume fraction of the void within its cell (or shortly the porosity) is set to be the same as the porosity of the whole body, namely

$$f = \frac{V^{(c)}}{V^{(c)} + V^{(m)}} = \frac{\sum V^{(c)}}{\sum V} \quad (\sum = \text{sum over all cells}). \tag{27}$$

As soon as the load is applied, the body starts to creep. In view of the expansion/contraction of the voids, the porosity is continuously changed (increased under tension and decreased under compression) as are the dimensions of the cell itself. In the "self-consistent" approach the interaction between the voids is gained by affecting the global material response (namely the viscosity $\eta(\bar{\varepsilon})$) as if the material behaves homogeneously with the properties of the representative cell with the void. In specific terms, the time variation of the average creeping rate of the overall body, $\dot{\bar{\varepsilon}}$, is continuously resolved and modified by η. This average creeping rate is defined in terms of the current porosity, f, the average matrix creeping rate $\dot{\bar{\varepsilon}}^{(m)}$ and the local void creeping rate $\dot{\bar{\varepsilon}}^{(c)}$ in a rule-of-mixtures-like form as

$$\dot{\bar{\varepsilon}} = \dot{\bar{\varepsilon}}^{(m)}(1-f) + \dot{\bar{\varepsilon}}^{(c)} f \tag{28}$$

where

$$\dot{\bar{\varepsilon}}^{(m)} = \left(\frac{\bar{\sigma}^{(m)}}{C}\right)^{1/n} \tag{29}$$

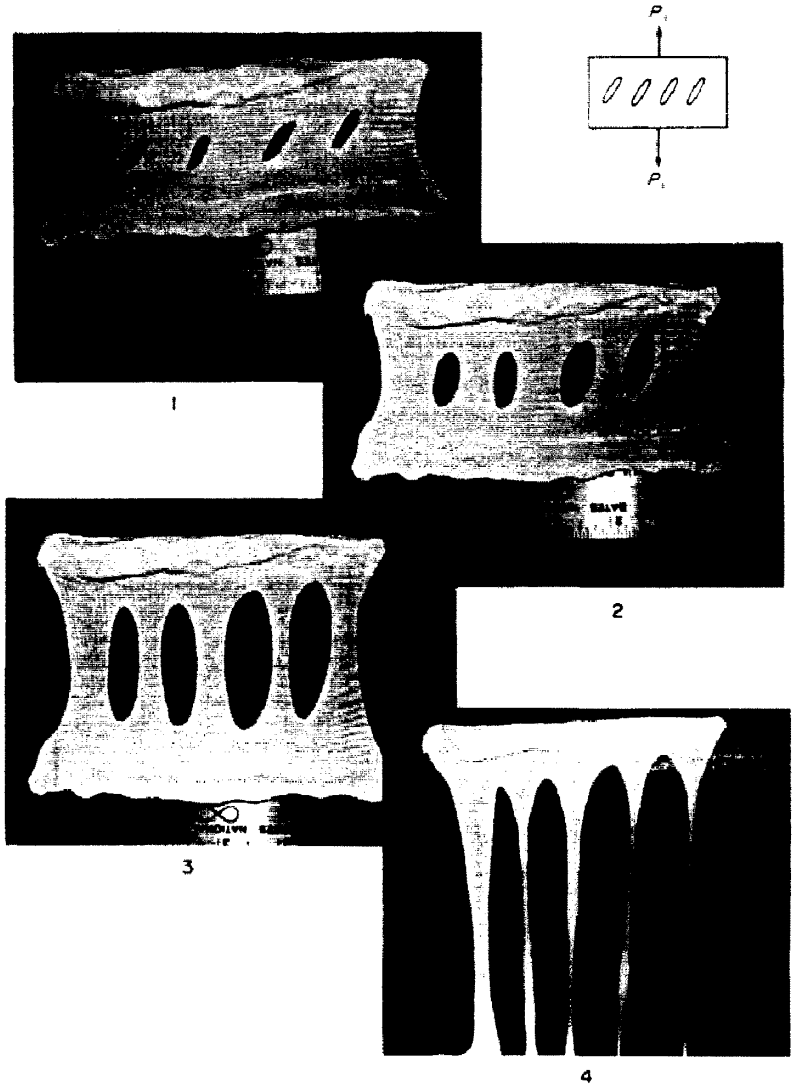

Fig. 3. Damage evolution sequence of voids expansion and rotation until coalescence.

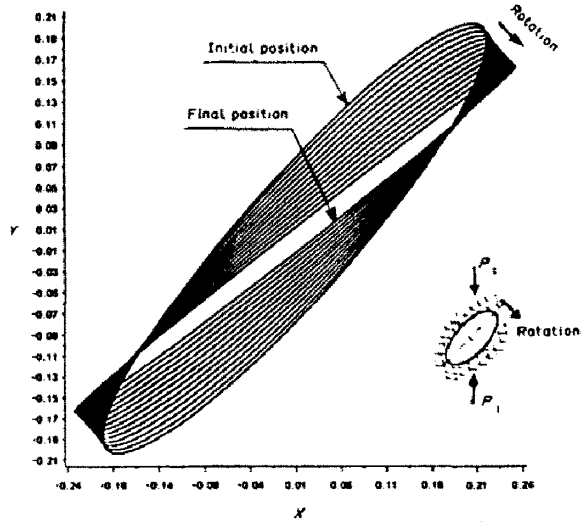

Fig. 4. The simultaneous void rotation and contraction during a power-law creep ($n = 0.5$) at a constant (vertical) compressive load, solved by eqns (21)–(25).

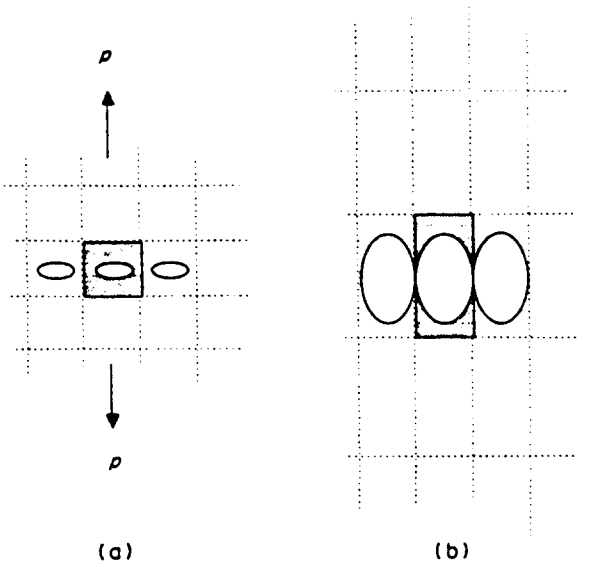

Fig. 5. A representative cell, (a) before the creep starts, (b) at the final rupture point.

is known from the creeping power law of eqn (1) and $\bar{\sigma}^{(m)}$ is the equivalent matrix stress (eqn (2)) based on the current stress components at the ligament. $\bar{\dot{\varepsilon}}^{(c)}$ is calculated from the current geometry and boundary motion of the void via eqn (10). The repeated updating of $\bar{\sigma}^{(m)}$ in eqn (29) calls for extensive use of the tensorial form of eqn (6), which is

$$\dot{\varepsilon}_{ij}^{(m)} = \frac{1}{2\eta^{(m)}} s_{ij}^{(m)} \tag{6}_1$$

where

$$\eta^{(m)} = (1/3)C(\bar{\varepsilon}^{(m)})^{n-1} \tag{7}_1$$

and

$$\varepsilon_{ij}^{(m)} = \int_0^t \dot{\bar{\varepsilon}}_{ij}^{(m)}\, dt. \tag{30}$$

With the matrix strain components of eqn (30) the new ligament dimensions are recomputed with associated modification of the stresses at the matrix $\sigma_{ij}^{(m)}$ (and hence $\bar{\sigma}^{(m)}$ in eqn (29)). By a proper account for the current growth of the void, the porosity, f, is updated by eqn (27) which affects the global creep rate $\dot{\bar{\varepsilon}}$ via eqn (28), and so forth at any time-step increment.

6. RESULTS AND DISCUSSION

The inception of rupture by void coalescence is reached in the suggested model at the point where the ligament cross-section (along either the X- or Y-axis, whichever comes first) shrinks to zero. Under vertical tension the computations lead to coalescence between adjacent voids (in the manner shown in Fig. 5) transverse to the load direction, as usually exhibited in testing[2]. As was observed in Fig. 3 and simulated by Fig. 2 each void undergoes creep with a substantial amount of rotation and expansion. Its ellipsoidal shape (m) is changed continuously but not monotonously. This seems to be more pronounced in ellipsoidal voids the initial angles of which with respect to the load (α_0) are larger. The void shape progressively becomes more circular (m is decreased in Fig. 6) but later on during the creep, it becomes more elongated ($m \to 1$) towards the direction of the load, which is in agreement with the series of photographs of Fig. 3. This fact has an immediate consequence

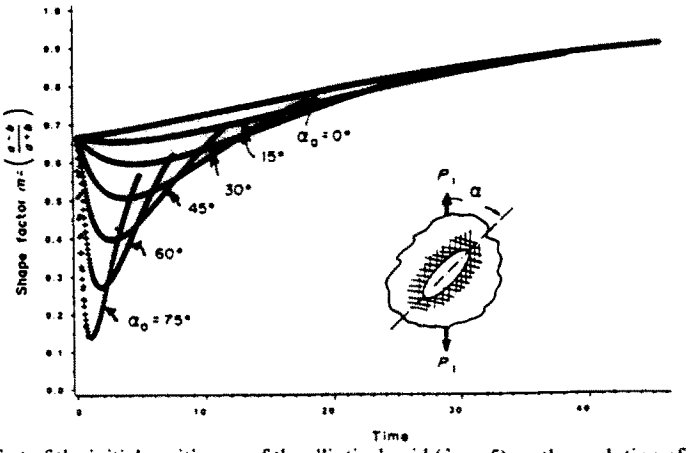

Fig. 6. The effect of the initial position α_0 of the elliptical void ($\lambda_0 = 5$) on the evolution of its shape. Similar "excursions" were actually observed (see Fig. 3).

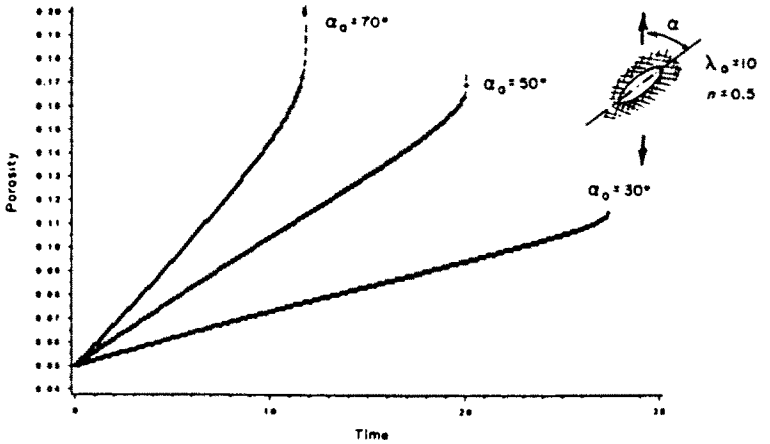

Fig. 7. Evolution of porosity of various initial voids positions. Different growth rates are exhibited ($\lambda_0 = 10$, $n = 0.5$, $f_0 = 5\%$).

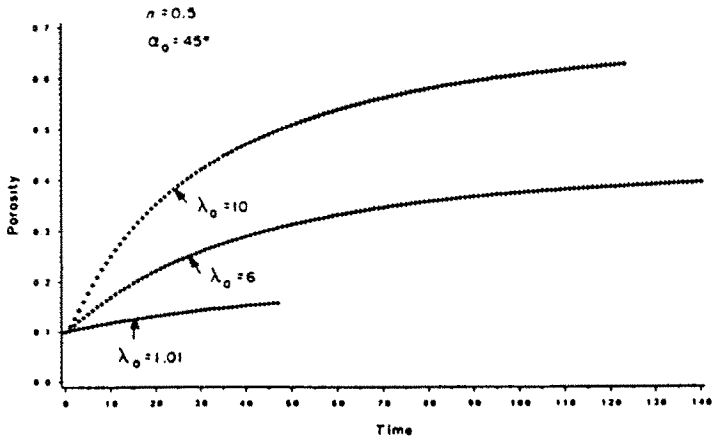

Fig. 8. Evolution of porosity at various aspect ratios λ_0. Different growth rates are exhibited ($\alpha_0 = 45°$, $n = 0.5$, $f_0 = 10\%$).

on the evolution rate of the damage (as shown on Fig. 7), namely, voids with higher α_0 decrease the creep–rupture lifetime. Much the same conclusion can be drawn with respect to the effect of the aspect ratio λ described in Fig. 8, where higher λ causes faster damage rate.

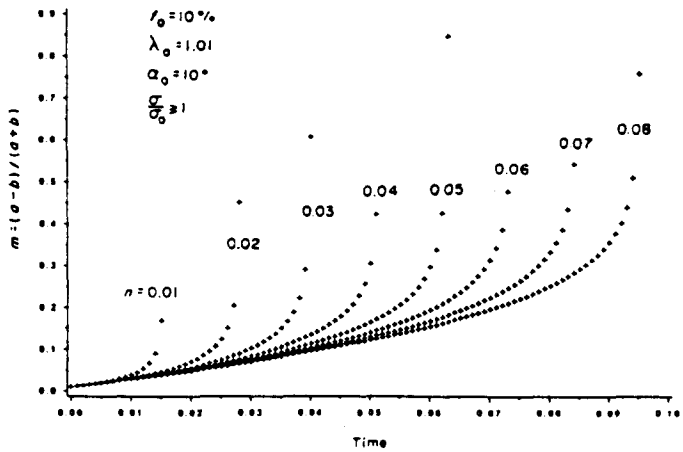

Fig. 9. The shape evolution at various rate sensitivity indexes. At moderately high load ($\sigma/\sigma_0 \geq 1$), the rate of change of the void shape is decreased with increasing the rate sensitivity index ($f_0 = 10\%$). Note that the data points are evaluated at a constant time interval so that the spacing of the cross points represents the rate of evolution.

The most common shape of initial voids in nature is circular (or nearly circular say, $\lambda_0 = 1.05$, which is equivalent to $m = 0.024$). Under such conditions the shape evolution and rotation for various rate sensitivity indexes is shown in Figs 9 and 10. The smaller the index the less the time for rupture. The damage growth is shown in Fig. 11 and the strain growth in Fig. 12 with the same trend—faster rupture at low sensitivity index (provided $P_1 > \sigma_0$). By properly normalizing these various creep histories with their respective time to rupture, t_r, and their respective porosity at rupture, f_r, a unified behavior of the damage and strain evolution emerges as a single curve, plotted in Figs 13 and 14 along with other damage theories. A relatively close resemblance is exhibited between the phenomenological damage models of Rabotnov–Kachanov (given in Ref. [11]), Dyson–McLean[12] and the present one. The conceptual difference between the theories of Rabotnov–Kachanov and Dyson–McLean and the present one is that the former need to postulate a damage-rate law (with pre-evaluated experimental constants) whereas the one suggested here needs only to pre-set the *initial* damage (i.e. the initial volume fraction of the voids). The former theories do not include the effect of the creeping rate on the damage evolution at constant load as was suggested here (e.g. 28). On the other hand the present model is somewhat deficient compared to the theories of Rabotnov–Kachanov and Dyson–McLean by being expressed in a semi-numerical fashion rather than analytically, thus less attractive for engineering applications. The similarity between the three models is that they are all *inherently non-steady under constant load.* That is to say that a strict *steady-state creep* cannot be simulated by any of the above theories. However, a nearly steady state is clearly feasible as exhibited for example, in Fig. 12. The small amount of deviation from steady-state creep rate reflects the role of the porosity evolution in enhancing the accumulation of plastic strain. This creep behavior appears only slightly sensitive to initial porosity at the range of, say, up to 10%.

The vast experimental data, collected by Woodford[13] is matched well with the suggested model (Fig. 15). It characterizes the ability of the present solution to predict the rupture strain of creeping metals. The scatter of the experimental data (and likewise in the model) stems from the fact that the strain at rupture (ε_f) is not so well defined as compared to the time to rupture (t_r). Close to the rupture time, the strain varies very rapidly as is always the case in the tertiary region of creep processes and hence the measurement of such terminal strain is highly ambiguous. By the same token, it is difficult to pick the correct value of ε_f in our theoretical simulation. For the purpose of consistency, one can set the rupture strain, ε_f, to be proportional to the Monkman–Grant[14] parameter, C_m ($C_m \equiv \dot{\varepsilon}_{mim} \cdot t_r$ where $\dot{\varepsilon}_{mim}$ is the minimum strain rate existing in the tertiary creep), such that $\varepsilon_f = \lambda_{CDT} \cdot C_m$. The proportionality factor, λ_{CDT} (having the physical meaning of creep damage tolerance[11, 15]), spans in most metals between 2 and 20[15]. We have chosen it

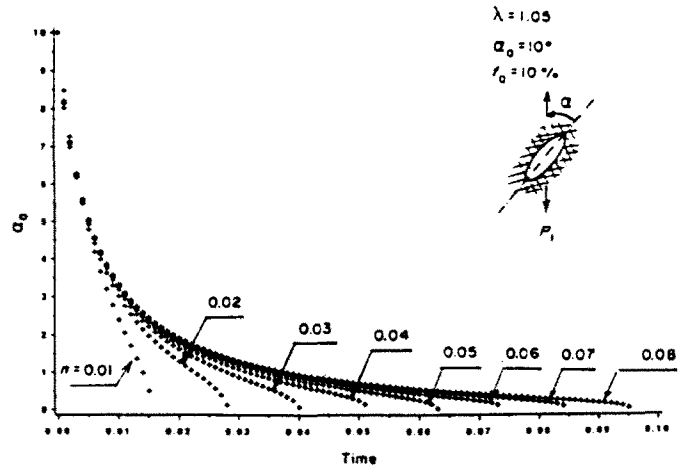

Fig. 10. The rotation rate of a void ($\lambda_0 = 1.05$, $f_0 = 10\%$) at various rate sensitivity indexes.

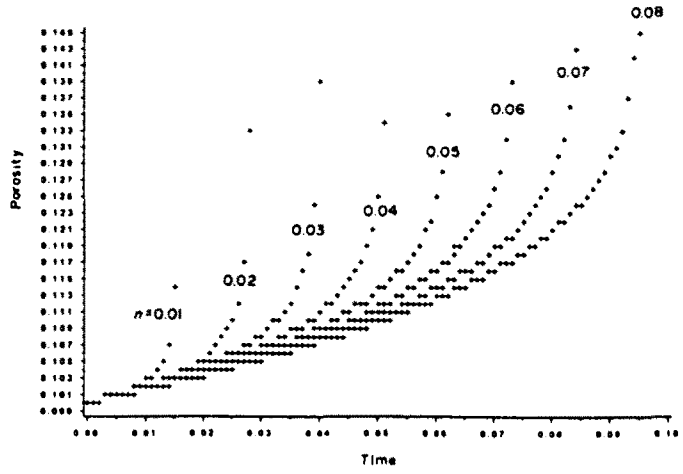

Fig. 11. Damage evolution (from initial porosity of 10%, $\alpha_0 = 10^\circ$, $\lambda_0 = 1.05$) until rupture for various rate sensitivity indexes.

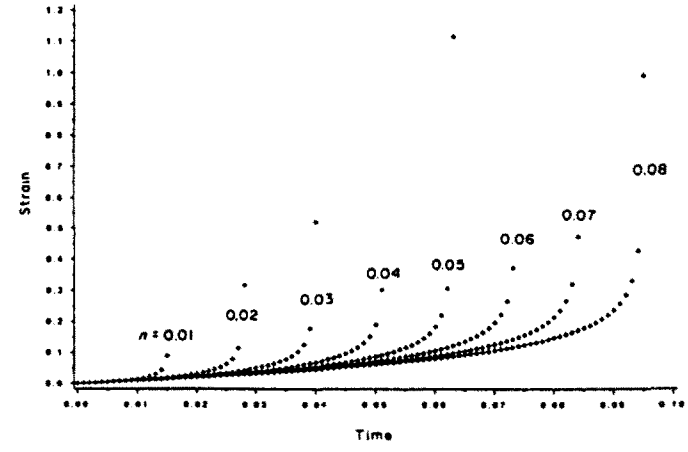

Fig. 12. The far field strain history for various rate sensitivity indexes.

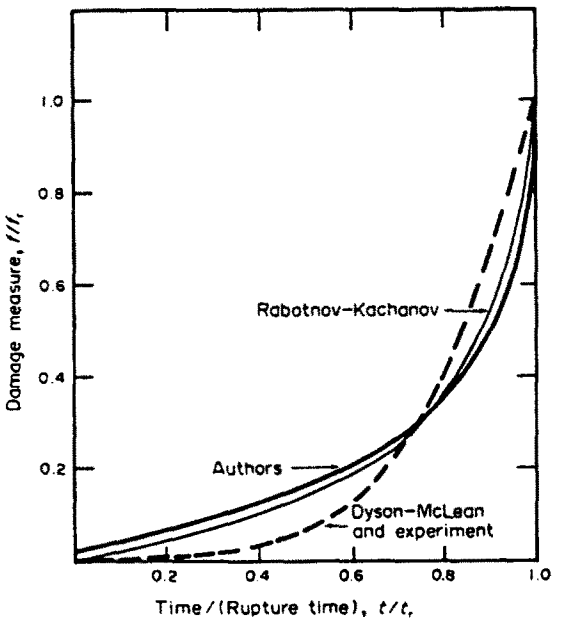

Fig. 13. Evolution of damage during power-law creep. Comparison between various models.

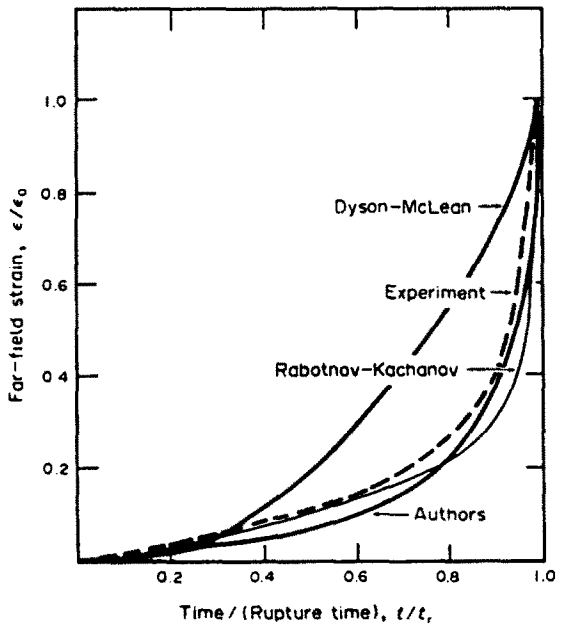

Fig. 14. Evolution of strain during power-law creep. Comparison between various models.

as 8 to resemble other works[11, 12]. At low porosity (till, say, 10%) and low rate sensitivity index (till, say, 0.1), the Monkman-Grant parameter appears to be close to $n(1-f_0)$, hence a "quick" prediction of rupture strain is approximately $\varepsilon_f \simeq 8n(1-f_0)$. For higher values of n, the time to rupture is longer, and C_m takes somewhat higher values in conjunction with the damage growth f.

The important evidence of the *induced anisotropy* in the mechanical behavior of the creeping solid due (probably) to the preferred orientation of the rotated voids, is still not incorporated in the present model. However, some other by-products as, for instance, void closure under compression, the effect of hydrostatic pressure, the material response to biaxial loading at various proportions, etc. are essentially included in the suggested model but await parallel experiments for validation.

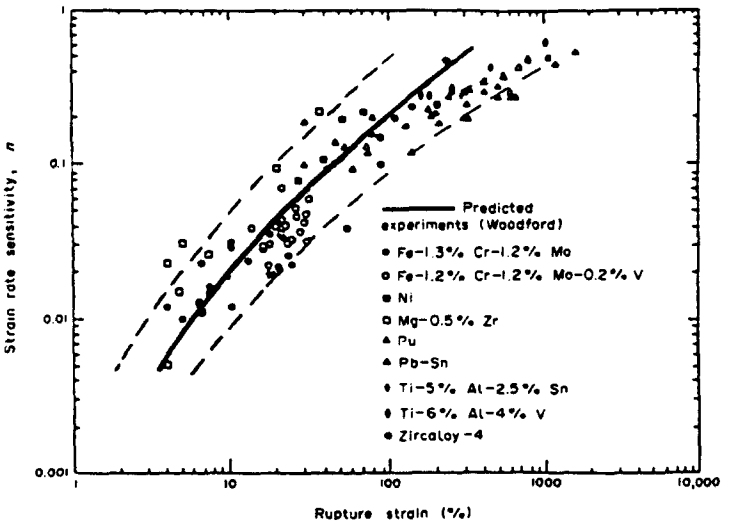

Fig. 15. Comparison between experiments (taken from Ref. [14]) and the present model. Correlation between strain rate sensitivity and rupture strain (ε_f) for a variety of materials is exhibited ($\lambda_0 = 1.05$, $f_0 = 2\%$).

Acknowledgements—This study was conducted at the Department of Materials Science and Engineering at Stanford University during the semi-sabbatical leave of the first author (J.T.) from Technion, Haifa, Israel. The work was funded by SIMA (Stanford Institute for Manufacturing and Automation).

REFERENCES

1. A. Needleman and J. R. Rice, Plastic creep flow in the diffusive cavitation of grain boundaries. *Acta Metall.* **28**, 1315–1332 (1980).
2. F. A. McClintock, A criterion for ductile fracture by growth of holes. *Trans. ASME*, Series E, *J. Appl. Mech.* **35**, 303–371 (1968).
3. J. R. Rice and D. M. Tracey, On the ductile enlargement of voids in triaxial stress field. *J. Mech. Phys. Solids* **17**, 201–217 (1969).
4. C. Berg, Deformation of fine cracks under high pressure and shear. *J. Geophys. Res.* **70**(14), 3447–3452 (1965).
5. B. Budiansky, J. W. Hutchinson and S. Slutsky, Void growth and collapse in viscous solids. In *Mechanics of Solids* (Edited by H. G. Hopkins and M. J. Sewell), pp. 13–45. Pergamon Press, Oxford (1982).
6. F. A. McClintock, S. M. Kaplan and C. A. Berg, Ductile fracture by hole growth in shear bands. *Int. J. Fracture Mech.* **2**, 614–627 (1966).
7. M. J. DiMelfi and W. D. Nix, Hole growth in plane viscous creep including interacting effects. *Int. J. Solids Structures* **12**, 217–225 (1976).
8. M. A. Burke and W. D. Nix, A numerical analysis of void growth in tension creep. *Int. J. Solids Structures* **15**, 55–71 (1979).
9. N. I. Muskhelishvili, *Some Basic Problems in Mathematical Theory of Elasticity*. Noordhoof, Groningen, The Netherlands (1953).
10. J. Tirosh, On the tensile and compressive strength of solids weakened (strengthened) by an inhomogeneity. *Trans. ASME*, Series E, *J. Appl. Mech.* **99**(3), 449–454 (1977).
11. F. A. Leckie and D. R. Hayhurst, Constitutive equations for creep rupture. *Acta Metall.* **25**, 1059–1070 (1977).
12. B. F. Dyson and D. McLean, Creep of nimonic 80A in torsion and tension. *Metal Sci.* **11**, 37–45 (1977).
13. D. A. Woodford, Strain-rate sensitivity as a measure of ductility. *Q. Trans. ASM* **62**, 291–293 (1969).
14. F. C. Monkman and N. J. Grant, An empirical relationship between rupture life and minimum creep rate in free-rupture tests. *Proc. ASTM* **56**, 593–620 (1956).
15. M. F. Ashby and B. F. Dyson, Creep damage mechanics and micromechanisms. *NPL Publ., DMA (A)* **77**, March (1984).